Applied Clay Science 257 (2024) 107447

Contents lists available at ScienceDirect

Applied Clay Science

journal homepage: www.elsevier.com/locate/clay

Technical note

Controlling clay slips with a process vibrational viscometer

Alejandro Ansón-Casaos [a,*], José-María Berges [a], José Carlos Ciria [b], Wolfgang K. Maser [a], Ana M. Benito [a], Jean-Marie Duboys [c]

[a] Instituto de Carboquímica, ICB-CSIC, Miguel Luesma Castán 4, 50018 Zaragoza, Spain
[b] Department of Computer Science and Systems Engineering (DIIS), University of Zaragoza, María de Luna 1, 50018 Zaragoza, Spain
[c] SOFRASER S.A.S., 15 rue Nobel, 45700 Villemandeur, France

ARTICLE INFO

Keywords:
Clay dispersion
Ceramic slurry
Shear thinning
Thixotropic behavior
Vibratory viscometer
Sanitary ware

ABSTRACT

The apparent viscosity of concentrated clay dispersions is a key control parameter in the ceramic industry, particularly in the manufacture of sanitaryware. Slips, the final industrial dispersions, are complex in their rheological behavior, featuring non-Newtonian flow and thixotropy. In this work, a resonance vibrating-rod viscometer (VRV) was utilized to evaluate the viscosity evolution over time, showing advantages over a classical rotational viscometer. Notably, while both viscometers were sensitive to small quantities of a deflocculant, the VRV effectively described the typical increase in the viscosity of clay dispersions at rest (thixotropy), the experimental data being properly fitted by a phenomenological model. As a relevant technical aspect, the superior suitability of the VRV for in-line process control was highlighted in the continuous monitoring of stirred clay dispersions and slip casting in plaster moulds. Additionally, a fitting model was developed to elucidate viscosity evolution during the casting process. In summary, this study underscores the versatility of the VRV as a control instrument in the sanitaryware industry.

1. Introduction

Clay materials are the basis of ceramic industries fabricating tiles, sanitaryware, fireclay, and porcelain (Burst, 1991). However, the manufacture of sanitary products, such as toilets and sinks, suffers from material and energy losses due to process failure, affecting up to 30% of the produced units (Fortuna, 2000). A main cause of failure is the variability in the composition of raw materials, arising from their natural or recycled origin (Stathis et al., 2004; Marinoni et al., 2011; Li et al., 2015; Ozturk et al., 2022; Bernasconi et al., 2023). These inconsistences represent substantial economical losses, which subsequently increase the final product prices. Unfortunately, the elevated cost renders toilets unaffordable for many individuals in underdeveloped regions, resulting in high ratios of disease transmission. Therefore, process and quality control throughout the fabrication chain of the sanitaryware industry faces particular challenges and needs to be improved (Pagani et al., 2010; Desole et al., 2024).

Clays are typically processed in concentrated aqueous dispersions (densities of 1.3–1.6 g·cm^{-3}) referred as slurries or slips, which are formulated by combining either raw materials coming directly from the mine or pre-processed clays with water into large mixing tanks (Silvestri et al., 2020). The preparation of clay slurries requires high-power stirring for a duration, ranging from 1 to 6 h, alongside the addition of specific deflocculants, such as sodium silicate (Sakar-Deliormanlı and Yayla, 2004; Ma, 2011; Konduri and Fatehi, 2017) to disperse clay particles and modulate viscosity, allowing for easier flow in pipes, pressing, filtering or casting. In addition to the clay component, which provides plasticity, sanitary slips incorporate quartz, feldspar, kaolin, and often chamotte (fired clay) reaching quite high densities of nearly 2 g·cm^{-3}. Once all the components are well-mixed, the slips are stored in maintenance tanks until they are poured into moulds for shaping the sanitary products. Next, the as-prepared bodies are dried, covered with glaze, and finally sintered at temperatures ranging from 1200 to 1300 °C (Baccarin et al., 2023).

Quality control in ceramic slips mainly relies on viscosity measurements, which are typically performed using flow cups (often Ford cups), torsional viscometers, or rotational viscometers. The rheological analysis of ceramic slips is complex, featuring particular non-Newtonian and time-dependent behaviors that complicate characterization (Gutiérrez et al., 2000). Moreover, slips show thixotropy, i.e. the viscosity increases over time at rest, and decreases under stirring (Chavan et al., 1975; Larson and Wei, 2019). The viscosity of sanitary slips increases by

* Corresponding author.
E-mail address: alanson@icb.csic.es (A. Ansón-Casaos).

https://doi.org/10.1016/j.clay.2024.107447
Received 27 March 2024; Received in revised form 27 May 2024; Accepted 31 May 2024
Available online 8 June 2024

Table 1
Crystal phase composition of the raw clay from XRD (Rietvel refinement with Brindley correction).

Crystal Phase	Generic composition	Phase composition [mass %]
Illite	$KAl_2Si_3AlO_{10}(OH)_2$	28.7
Kaolinite	$Al_2Si_2O_5(OH)_4$	19.8
Quartz	SiO_2	17.4
Rutile	TiO_2	1.1
Amorphous	–	33.0

10–30% after 1–5 min at rest, and reaches up to 10-fold higher values after 1 h of slow stirring (Fortuna, 2000). The fluidity and thixotropy of slips are influenced by various parameters, including composition, processing history, and ambient conditions (Rastelli et al., 2008).

In this context, the use of a resonant vibrational viscometer is a novel approach for the in-situ control of clay-slip viscosity and thixotropy. Among the different types of vibrational viscometers available in the market (Ji et al., 2012), a vibrating-rod viscometer (VRV) offers advantageous characteristics for measurements in industrial processes (Kawatra and Bakshi, 1995). Operating at its resonance frequency, the VRV provides optimal signal-to-viscosity ratio, and exhibits excellent tolerance to variations in the fluid level. Moreover, its resonance frequency shows minimal sensitivity to external vibrations in industrial environment, while operating at around 300 Hz ensures a limited influence of shear rate on viscosity data.

In this work, the performance of a VRV in a concentrated clay dispersion was first explored, comparing its results with data obtained from a widely-used rotational viscometer. The different measurement principles of both devices, a metallic rod vibrating perpendicularly to its axis and a rotating spindle respectively, led to specific response trends, which needed to be comprehended. In detail, the signal evolution with time was tracked to evaluate the impact of thixotropy on apparent viscosity. Subsequently, the VRV was tested in two case studies: i) continuous monitoring of a clay dispersion under stirring; and ii) continuous monitoring of a sanitary slip during its conformation inside a plaster mould. Furthermore, fitting models were applied to conceptualize the observed trends at the molecular and particle level.

2. Experimental

Clay materials were provided by Euroarce (Ariño, Teruel, Spain), specifically: i) a raw clay in the form of crushed stone, which was a mixture from several Euroarce mines in the province of Teruel; and ii) a standard sanitary ceramic slip (density $\rho = 1.96$ g·cm^{-3}), composed by the raw clay, kaolin, silica and feldspar in roughly equal weight ratios. The vibrating-rod viscometer (VRV) was a MIVI system from Sofraser (Villemandeur, France), with electronics 9000 and processor 9710. This VRV is based on the principle of a rod vibrating at its resonance frequency (Beaudoin and Maronne, 1983). Other details about equipment, preparation of clay dispersions and measurements are provided in the Supplementary Material.

3. Results and discussion

The raw clay exhibits the characteristic elemental composition and mineral phases (Table 1 and Supplementary Material) that are observed in other clays for sanitaryware manufacture (Tunçel and Özel, 2012; Genç et al., 2022). Moreover, the typical flow curve of Ariño clay dispersions, performed with a rotational rheometer, revealed the characteristic non-Newtonian shear-thinning behavior of ceramic slurries (Amorós et al., 2002; Amorós et al., 2010), where viscosity (η) strongly decreases with stirring shear rate ($\dot{\gamma}$) (Fig. S2, Supplementary Material).

3.1. Clay dispersion at rest

To evaluate the applicability of the VRV in monitoring clay viscosity, dispersions with well-defined densities and quantities of sodium silicate (< 0.7 wt%) were examined. Sodium silicate deflocculant is a common additive in industry, aimed at stabilizing the dispersion and tuning its fluidity through an increase in the electrolytic conductivity (Fig. S3, Supplementary Material) that improves repulsion forces between particles. The VRV steadily provided the evolution of viscosity with time at a fixed shear rate. To facilitate comparison with the Brookfield rotational viscometer, parallel measurements with both instruments were performed (Fig. 1). Two notable differences clearly arose between them: i) the rotational viscometer registered considerably higher η values than the VRV, which likely came from the much higher $\dot{\gamma}$ value of the last one (2 and 300 s^{-1} respectively) (Chen and Lin, 2017); and ii) the evolution over a 30-min time period followed opposite trends. While the rotational viscometer returned a typical decreasing curve, the VRV indicated an increasing viscosity over time. This fact was not contradictory, but it reflected the different device working principles, as it will be discussed

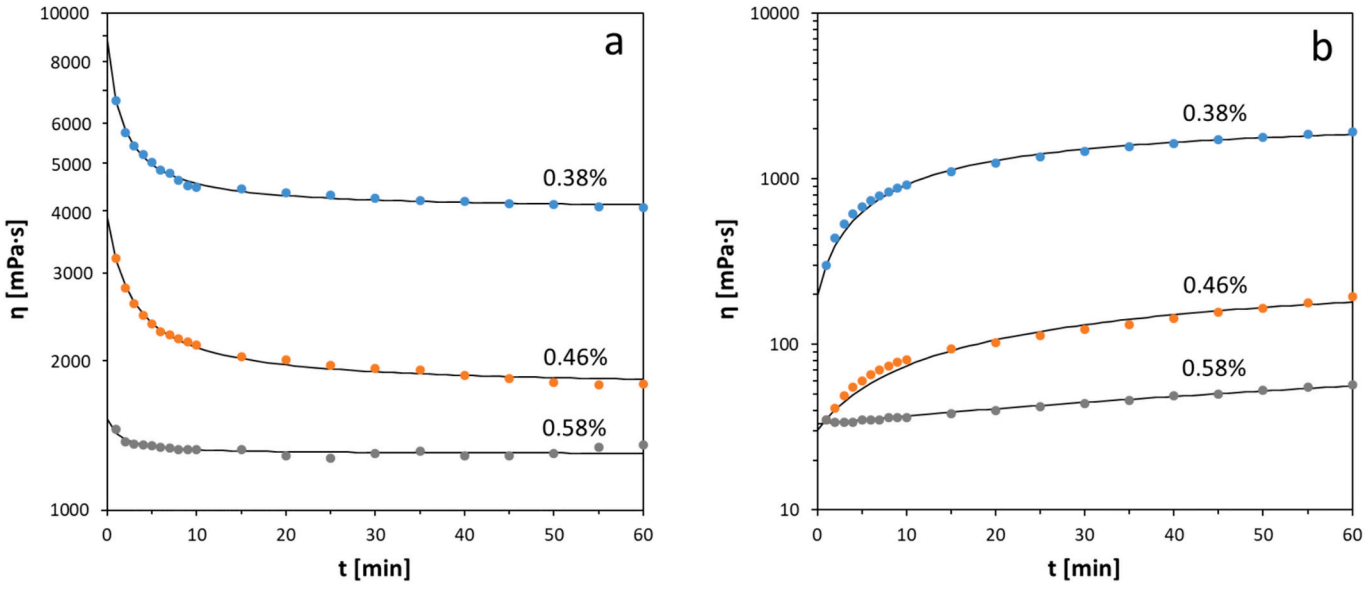

Fig. 1. Evolution of viscosity on formulated dispersions of the raw clay with $\rho = 1.55$ g·cm^{-3} and various loadings (wt%) of sodium silicate deflocculant, as obtained by measurements using: a) rotational viscometer; and b) VRV. Fitting curves follow Eq. 1.

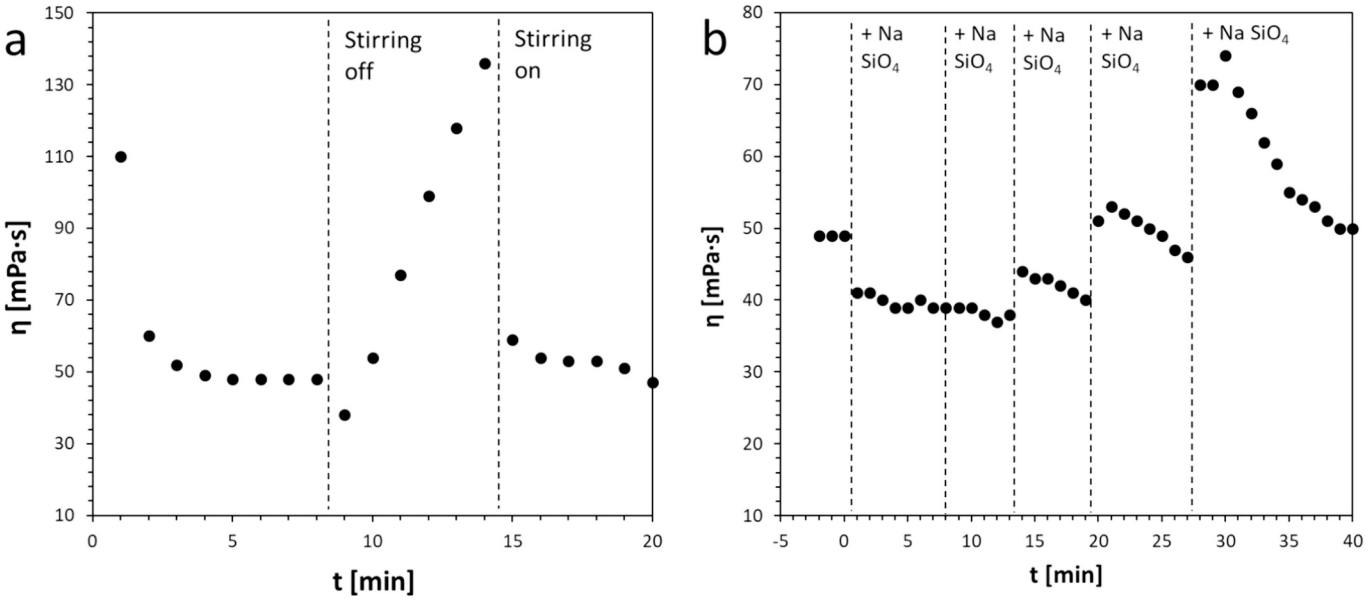

Fig. 2. Response of the VRV in a clay dispersion ($\rho = 1.55$ g·cm^{-3}, 0.44 wt% sodium silicate) under stirring at 1000 rpm: a) inserting a 5 min period of rest; and b) with subsequent additions of 1.3 mL of deflocculant sodium silicate.

in the following paragraphs. Moreover, both viscometers coherently interpreted that viscosity decreased as the quantity of sodium silicate deflocculant increased within the range of 0.38–0.58 wt%. Accordingly, deflocculation curves (η as a function of the silicate addition) could be plotted (Fig. S4, Supplementary Material).

Curves of viscosity vs. time (η vs. t) reflect changes in the fluid structure. At rest, dense clay dispersions create an internal structure through inter-particle and electrostatic interactions, resulting in a gradual increase in viscosity with time, i.e. thixotropy (de Souza Mendes, 2009; Larson and Wei, 2019; Fazilati et al., 2021). On the contrary, viscosity decreases when the fluid is stirred, disrupting the internal structure. Additionally, the viscometer probe itself induces continuous shaking and distortion of the fluid structure to some extent. The decreasing trend that is observed with the rotational viscometer was fitted by Nguyen et al. (1998) and Nasser and James (2008) applying a phenomenological kinetic model. They derived the following equation:

$$\left(\frac{\eta - \eta_e}{\eta_0 - \eta_e}\right)^{1-p} = (p-1)kt + 1 \quad (1)$$

where η_0 is the viscosity at $t = 0$, η_e the viscosity at a final equilibrium state ($t = \infty$), p is the kinetic order, and k is the rate constant of structural breakdown. Typically, the value of p can be reasonably taken as 2. In fact, it was confirmed that Eq. 1 satisfactorily fitted curves from the rotational viscometer (Fig. 1.a). Moreover, Eq. 1 was also able to adequately describe the increasing trends observed with the VRV (Fig. 1.b). Typical fitting values of k fell in the range of 0.1–1 min^{-1} for the rotational viscometer data, and 0.01–0.5 min^{-1} for the VRV. The change in the order of magnitude clearly indicated different kinetic regimes caused by the measurement method.

The decreasing curve η vs. t of the rotational viscometer (Fig. 1.a) mainly reflected the shaking effect caused by the spindle rotating in the fluid. In the vicinity of the spindle, fluidity increases. Conversely, the increasing trend observed with the VRV is attributed to fluid structuring, and it correlates with the real thickening (thixotropy). The VRV induced a low level of deformation in the clay dispersion, in agreement with previous measurements using a different type of laboratory vibrational viscometer (Ji et al., 2012). A further assessment of thixotropy with the VRV, as well as the effect of clay dispersion density, is discussed in the Supplementary Material.

3.2. Stirred clay dispersion

In industry, clay dispersions and slips are conditioned and stored in tanks under moderate or gentle stirring. Monitoring viscosity is important to assess the impact of material additions and ageing time, thereby preventing excessive thickening or thinning. It is here proposed that the VRV can effectively serve for process control in slip tanks, avoiding the problems of sampling and off-line analysis.

As a proof of concept, the VRV response was tested in a raw clay dispersion of $\rho = 1.55$ g·cm^{-3} and optimal sodium silicate ratio of 0.44 wt% under stirring (Fig. 2). The η value of this clay dispersion under 1000 rpm was approximately 50 mPa·s. When the stirrer was stopped, the η value increased until nearly 140 mPa·s in 5 min, according to a thixotropic behavior. Upon restarting the stirrer, the η value rapidly reverted to its initial level of 50 mPa·s (Fig. 2.a). Thus, the VRV demonstrated fast responsiveness to the stopping and restarting of stirring, allowing the in-line evaluation of thixotropy.

Moreover, the viscometer responded immediately to the addition of small quantities of the deflocculant solution (Fig. 2.b), each one of approximately 1 mL (1.3 g, 0.04 wt% of the whole mixture). The first extra additions did not change substantially the η value. However, subsequent additions tended to increase η value, indicating that the ratio of deflocculant exceeded the optimal (the clay slurry was over-deflocculated). It was also verified that controlled additions of water (10 mL, 0.7 wt% of the mixture, not shown in Fig. 2 for simplicity) resulted in measurable decreases in η value of approximately 5 mPa·s. Therefore, the VRV emerges as a promising tool providing relevant real-time information into the process dynamics, facilitating precise control over clay dispersion viscosity and composition adjustments in industrial clay manufactures.

3.3. Slip casting

The shaping of sanitaryware products takes place in porous moulds, which are typically made of plaster or synthetic resins (Ochoa et al., 2017). The moulds are filled with slip and left to rest or sometimes pressurized. During the casting process, water is progressively extracted from the slip through the mould pores, while a solid deposit forms on the inner wall (Mikhalev et al., 2007). Casting period ranges from 10 to 20 min, in pressurized systems, to several hours in normal moulds. Next,

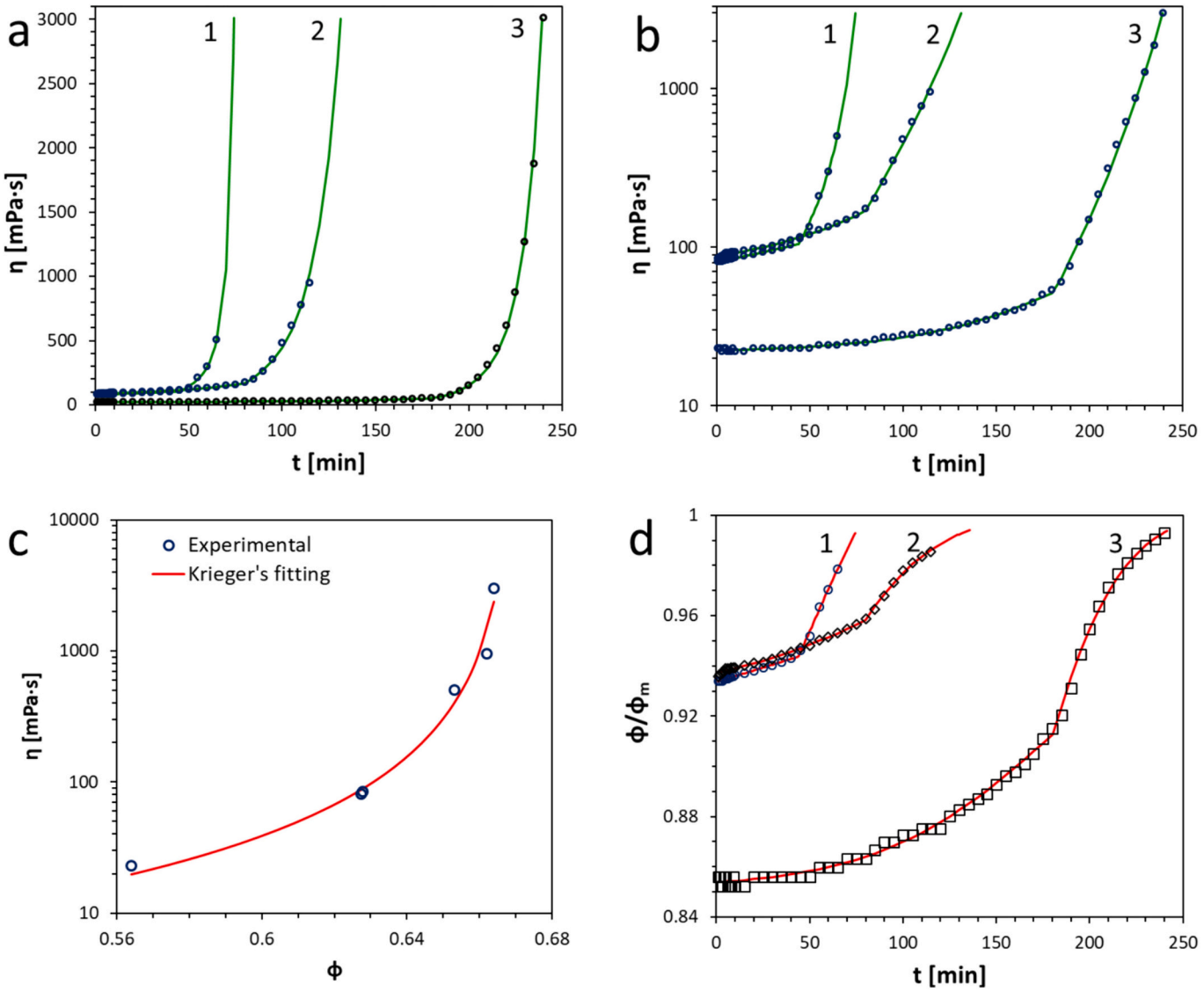

Fig. 3. VRV data from casting processes in a plaster mould with a ceramic slip at $\rho = 1.96$ g·cm^{-3} (Experiments 1 and 2) and $\rho = 1.81$ g·cm^{-3} (Experiment 3): a) Linear plot of η vs. t; b) Logarithmic plot of η vs. t; c) Experimental data of the packing factor (ϕ) and fitting to the Krieger's equation (Eq. 3); d) Evolution of ϕ calculated from Eqs. 2 and 3.

the excess slip is removed and the mould is open.

As a proof of concept, three casting experiments were conducted using a plaster mould, under ambient conditions (Fig. 3). Experiments 1 and 2 were performed different days with the as-received sanitary slip at $\rho = 1.96$ g·cm^{-3}, while Experiment 3 involved diluting the slip with water to $\rho = 1.81$ g·cm^{-3}. In all three experiments, the slip viscosity increased during the casting period because of the thixotropic thickening and the loss of water (Fig. 3.a). The end of the process correlated with a steep increase in η value, which resembled other thickening, stiffening and hardening processes observed in various systems, such as organic plastic gels, inorganic xerogels, adhesives, plaster, and cement (Nitta et al., 1999; Padding et al., 2012; Ochoa et al., 2017; Ji et al., 2017; Maki, 2019). It became apparent that the length of the casting period depended not only on known slip characteristics, such as density, but also on other conditions (compare Experiments 1 and 2 in Fig. 3.a), such as temperature, ambient, mould humidity, or slip history, that are rather challenging to control, particularly in industrial environments.

During slip casting, viscosity followed two regimes: first, it increased relatively slowly, while over long periods it increased fast. Both regimes were separated by an inflection point, which was particularly well observed in the logarithmic plot (Fig. 3.b). This dual trend was in good agreement with previous studies (Nitta et al., 1999; Amorós et al., 2002; Ochoa et al., 2017; Maki, 2019). Here, it was proposed that the pattern could be effectively modeled by the following function:

$$\eta(t) = \begin{cases} \eta_0 + \alpha_0\left(e^{\lambda_0 t} - 1\right), t \le t_0 \\ \alpha_1 (t_m - t)^{-\lambda_1}, t \le t_0 \end{cases} \quad (2)$$

where η_0 is the viscosity at $t = 0$; t_0 is the inflection point; t_m is the time when the viscosity becomes infinite; and λ_0, λ_1, α_0 and α_1 are the other fitting parameters. The fitting curves were shown in Fig. 3.b, and the relevant fitting parameters were included in Table 2. Notably in Eq. 2, η (t) is a continuously differentiable function of time except at the

Table 2
Relevant fitting parameters for slip casting experiments (Fig. 3) applying Eq. 2.

Parameter	Experiment 1	Experiment 2	Experiment 3
η_0 [mPa·s]	80.4 ± 0.4	88.1 ± 0.4	22.4 ± 0.1
t_0 [min]	44.3 ± 0.3	79.6 ± 0.5	181.2 ± 0.4
t_m [min]	79.8 ± 1.2	215.7 ± 19.6	304.9 ± 3.4

inflection point t_0, where its derivative changes abruptly and seems to undergo a discontinuity: such a behavior is reminiscent of a phase transition.

For a deeper understanding, results were also correlated with the packing factor (ϕ) of the particle dispersion. Amorós et al. (2002) observed that ceramic slips follow the Krieger's equation, which stablishes a relationship between the relative viscosity and the packing factor (ϕ):

$$\frac{\eta}{\eta_s} = \left(1 - \frac{\phi}{\phi_m}\right)^{-[\eta]\phi_m} \quad (3)$$

where η_s is the viscosity of the solvent (water), $[\eta]$ the intrinsic viscosity, and ϕ_m the maximum packing factor. The packing factor (ϕ) can be calculated as the volume ratio of solid particles in the dispersion. Thus, ϕ values at the beginning and the end of the casting experiments were approximated from experimental data, including slip density, specimen volume, specimen weight at the end of the casting experiment, and specimen weight after totally drying in an oven at 90 °C. Remarkably, the data (ϕ vs. η) were well fitted to Eq. 3 (Fig. 3.c), with the fitting parameters being: $\phi_m = 0.669 \pm 0.01$ and $[\eta] = 2.416 \pm 0.058$.

Finally, from Eqs. 2 and 3, the ϕ value was calculated as a function of time (Fig. 3.d). Around the inflection point t_0, the ϕ value increases fast, which can be tentatively associated with the accommodation of irregular particles suspended in the fluid phase into an ordered nearly solid bulk structure.

4. Conclusions

The comprehensive analysis conducted in this study sheds light on various aspects of clay dispersions and their behavior during processing, casting, and moulding into sanitaryware products. It notably highlights the ability of the VRV to accurately assess changes in the composition and thixotropic behavior, particularly the observed viscosity increase during rest periods. The rapid response of VRV to viscosity changes underscores its potential for real-time process control in slip tanks, offering a practical solution for monitoring and adjusting viscosity during manufacturing processes, thereby optimizing product quality and minimizing production inefficiencies. In contrast, off-line sampling and analysis leads to delays in process monitoring and intervention.

Distinct viscosity trends were observed during slip casting, characterized by an initial slow increase followed by a rapid escalation over time. A mathematical model is proposed that effectively describes the dual viscosity regime, providing insights into the phase transition-like behavior at the inflection point, and uncovering a clear relationship between viscosity and particle arrangement.

While rotational viscometers are widely used in various industries, including tradicional ceramics, the VRV offers unique advantages, particularly in applications requiring precise continuous monitoring and rapid response. Its adaptability to different process conditions and environments makes it a versatile tool for process control in the ceramic industry, in particular for slip conditioning and casting in sanitaryware production.

CRediT authorship contribution statement

Alejandro Ansón-Casaos: Writing – original draft. **José-María Berges:** Conceptualization. **José Carlos Ciria:** Data curation. **Wolfgang K. Maser:** Funding acquisition. **Ana M. Benito:** Writing – review & editing. **Jean-Marie Duboys:** Resources.

Declaration of competing interest

The authors declare that they have no known competing financial interests or personal relationships that could have appeared to influence the work reported in this paper.

Data availability

Data will be made available on request.

Acknowledgements

Special thanks are directed to Ms. Noelia Omedas, manager of the Euroarce plant at Ariño (Teruel, Spain), Mr. Philippe Burg for his collaboration from Sofraser and Dr. Ramón Murillo from ICB-CSIC. Financial support from Gobierno de Aragón (DGA) under project T03_23R (Grupo de Investigación Reconocido) is acknowledged.

Appendix A. Supplementary data

Supplementary data to this article can be found online at https://doi.org/10.1016/j.clay.2024.107447.

References

Amorós, J.L., Sanz, V., Gozalbo, A., Beltrán, V., 2002. Viscosity of concentrated clay suspensions: effect of solids volume fraction, shear stress, and deflocculant content. Br. Ceram. Trans. 101, 185–193. https://doi.org/10.1179/096797802225003992.

Amorós, J.L., Orts, M.J., Mestre, S., Garcia-Ten, J., Feliu, C., 2010. Porous single-fired wall tile bodies: Influence of quartz particle size on tile properties. J. Eur. Ceram. Soc. 30, 17–28. https://doi.org/10.1016/j.jeurceramsoc.2009.08.001.

Baccarin, L.I.P., Bielefeldt, W.V., Bragança, S.R., 2023. Prediction of glass phase viscosity in firing traditional ceramics and porcelain tiles with waste glass powder. Open Ceram. 15, 100417 https://doi.org/10.1016/j.oceram.2023.100417.

Beaudoin, P., Maronne, P., 1983. Viscosimètre à tige vibrante. FR2544496.

Bernasconi, A., Bernasconi, D., Francescon, F., Sartori, R., Pavese, A., 2023. Fine Fireclay (FC) technological properties and mineralogy by tuning body composition and raw materials particle size distribution. Ceram. Int. 49, 28224–28232. https://doi.org/10.1016/j.ceramint.2023.06.077.

Burst, J.F., 1991. The application of clay minerals in ceramics. Appl. Clay Sci. 5, 421–443. https://doi.org/10.1016/0169-1317(91)90016-3.

Chavan, V.V., Deysarkar, A.K., Ulbrecht, J., 1975. On Phenomenological characterisation of thixotropic behaviour. Chem. Eng. J. 10, 205–214. https://doi.org/10.1016/0300-9467(75)80038-4.

Chen, C.-T., Lin, C.-W., 2017. Stiffening behaviors of cement pastes measured by a vibrational viscometer. Adv. Civ. Eng. Mater. 6, 53–64. https://doi.org/10.1520/ACEM20160061.

de Souza Mendes, P.R., 2009. Modeling the thixotropic behavior of structured fluids. J. Non-Newtonian Fluid Mech. 164, 66–75. https://doi.org/10.1016/j.jnnfm.2009.08.005.

Desole, M.P., Fedele, L., Gisario, A., Barletta, M., 2024. Life Cycle Assessment (LCA) of ceramic sanitaryware: focus on the production process and analysis of scenario. Int. J. Environ. Sci. Technol. 21, 1649–1670. https://doi.org/10.1007/s13762-023-05074-6.

Fazilati, M., Ingelsten, S., Wojno, S., Nypelö, T., Kádár, R., 2021. Thixotropy of cellulose nanocrystal suspensions. J. Rheol. 65, 1035–1052. https://doi.org/10.1122/8.0000281.

Fortuna, D., 2000. Ceramic Technology Sanitaryware. Grupo Editoriale Faenza Editrice SPA.

Genç, Ş.C., Kayacı, K., Yıldırım, Y., 2022. Mineralogical and technological properties of the Konya clays, Central Turkey. J. Therm. Anal. Calorim. 147, 1887–1897. https://doi.org/10.1007/s10973-020-10463-x.

Gutiérrez, C., Sánchez-Herencia, A.J., Moreno, R., 2000. Plastic or pseudoplastic? Methods for determining and analising the yield stress of ceramic slips. Bol. Soc. Esp. Cerám. Vidrio 39, 105–117.

Ji, H., Lim, H.M., Chang, Y.-W., Lee, H., 2012. Comparison of the viscosity of ceramic slurries using a rotational rheometer and a vibrational viscometer. J. Kor. Ceram. Soc. 49, 542–548. https://doi.org/10.4191/kcers.2012.49.6.542.

Ji, Y., Yang, Z., Shi, M., Tan, H., 2017. Effect of the particulate morphology of resin on the gelation process of PVC plastisols. J. Polym. Eng. 37, 757–764. https://doi.org/10.1515/polyeng-2016-0215.

Kawatra, S.K., Bakshi, A.K., 1995. On-line viscometry in particulate processing. Miner. Process. Extr. Metall. Rev. 14, 249–273. https://doi.org/10.1080/08827509508914126.

Konduri, M.K.R., Fatehi, P., 2017. Dispersion of kaolin particles with carboxymethylated xylan. Appl. Clay Sci. 137, 183–191. https://doi.org/10.1016/j.clay.2016.12.027.

Larson, R.G., Wei, Y., 2019. A review of thixotropy and its rheological modeling. J. Rheol. 63, 477–501. https://doi.org/10.1122/1.5055031.

Li, J., Liang, J., Wang, F., Wang, L., 2015. Effect of sepiolite fibers addition on sintering behavior of sanitary bodies. Appl. Clay Sci. 105–106, 231–235. https://doi.org/10.1016/j.clay.2014.10.017.

Ma, M., 2011. The dispersive effect of sodium silicate on kaolinite particles in process water: implications for iron-ore processing. Clay Clay Miner. 59, 233–239. https://doi.org/10.1346/CCMN.2011.0590302.

Maki, Y., 2019. Poly(N,N-dimethylacrylamide)-clay nanocomposite hydrogels with patterned mechanical properties. Colloid Polym. Sci. 297, 587–594. https://doi.org/10.1007/s00396-019-04486-6.

Marinoni, N., Pagani, A., Adamo, I., Diella, V., Pavese, A., Francescon, F., 2011. Kinetic study of mullite growth in sanitary-ware production by in situ HT-XRPD. The influence of the filler/flux ratio. J. Eur. Ceram. Soc. 31, 273–280. https://doi.org/10.1016/j.jeurceramsoc.2010.10.002.

Mikhalev, V.V., Serov, V.V., Vlasov, A.S., 2007. Effect of the physical properties of slip on the molding of commercial grade sanitary ware. Glas. Ceram. 64, 129–131. https://doi.org/10.1007/s10717-007-0033-4.

Nasser, M.S., James, A.E., 2008. Compressive and shear properties of flocculated kaolinite–polyacrylamide suspensions. Colloids Surf. A Physicochem. Eng. 317, 211–221. https://doi.org/10.1016/j.colsurfa.2007.10.021.

Nguyen, Q.D., Jensen, C.T.B., Kristensen, P.G., 1998. Experimental and modelling studies of the flow properties of maize and waxy maize starch paste. Chem. Eng. J. 70, 165–171. https://doi.org/10.1016/S0923-0467(98)00081-5.

Nitta, S.V., Jain, A., Wayner Jr., P.C., Gill, W.N., Plawsky, J.L., 1999. Effect of sol rheology on the uniformity of spin-on silica xerogel films. J. Appl. Phys. 86, 5870–5878. https://doi.org/10.1063/1.371605.

Ochoa, R.E., Gutiérrez, C.A., Rendón, J.C., Rodríguez, J.L., 2017. Effect of preparation variables of plaster molds for slip casting of sanitary ware. Bol. SECV 26, 263–272. https://doi.org/10.1016/j.bsecv.2017.06.001.

Ozturk, Z.B., Kunduracı, N., Binal, G., 2022. Influence of stone cutting waste addition on technological properties of ceramic sanitaryware bodies. Glas. Phys. Chem. 48, 570–575. https://doi.org/10.1134/S108765962210008X.

Padding, J.T., Mohite, L.V., Auhl, D., Schweizer, T., Briels, W.J., Bailly, C., 2012. Quantitative mesoscale modeling of the oscillatory and transient shear rheology and the extensional rheology of pressure sensitive adhesives. Soft Matter 8, 7967–7981. https://doi.org/10.1039/c2sm07443e.

Pagani, A., Francescon, F., Pavese, A., Diella, V., 2010. Sanitary-ware vitreous body characterization method by optical microscopy, elemental maps, image processing and X-ray powder diffraction. J. Eur. Ceram. Soc. 30, 1267–1275. https://doi.org/10.1016/j.jeurceramsoc.2009.11.008.

Rastelli, E., Salomoni, A., Fregni, A., Stamenkovic, I., 2008. Influence of calcium phosphate on rheological properties of sanitaryware slip. Adv. Appl. Ceram. 107, 76–82. https://doi.org/10.1179/174367608X263278.

Sakar-Deliormanlı, A., Yayla, Z., 2004. Effect of calcium hydroxide on slip casting behaviour. Appl. Clay Sci. 24, 237–243. https://doi.org/10.1016/j.clay.2003.04.001.

Silvestri, L., Forcina, A., Silvestri, C., Ioppolo, G., 2020. Life cycle assessment of sanitaryware production: a case study in Italy. J. Clean. Prod. 251, 119708 https://doi.org/10.1016/j.jclepro.2019.119708.

Stathis, G., Ekonomakou, A., Stournaras, C.J., Ftikos, C., 2004. Effect of firing conditions, filler grain size and quartz content on bending strength and physical properties of sanitaryware porcelain. J. Eur. Ceram. Soc. 24, 2357–2366. https://doi.org/10.1016/j.jeurceramsoc.2003.07.003.

Tunçel, D.Y., Özel, E., 2012. Evaluation of pyroplastic deformation in sanitaryware porcelain bodies. Ceram. Int. 38, 1399–1407. https://doi.org/10.1016/j.ceramint.2011.09.019.